JOURNAL OF MAGNETIC RESONANCE **135,** 535–540 (1998)
ARTICLE NO. MN981596

Cation Binding Induced Changes in ^{15}N CSA in a Membrane-Bound Polypeptide

F. Tian and T. A. Cross

Center for Interdisciplinary Magnetic Resonance, National High Magnetic Field Laboratory, Institute of Molecular Biophysics, Department of Chemistry, Florida State University, Tallahassee, Florida 32306-4005

Received April 21, 1998; revised August 26, 1998

Cation binding to the monovalent cation selective channel, gramicidin A, is shown to induce changes in the dipolar and chemical shift observables from uniformly aligned samples. While these changes could be the result of structural or dynamic changes, they are shown to be primarily induced by through-bond polarizability effects when cations are solvated by the carbonyl oxygens of the peptide backbone. Upon cation binding partial charges are changed throughout the peptide plane, inducing large changes in the $^{13}C_1$ chemical shifts, smaller changes in the ^{15}N chemical shifts, and even smaller effects for the ^{15}N–$^{13}C_1$ and ^{15}N–^{2}H dipolar interactions. These conclusions are substantiated by characterizing the ^{15}N chemical shift tensors in the presence and absence of cations in fast-frozen lipid bilayer preparations of gramicidin A.

The interpretation of changes in anisotropic chemical shifts is complicated by numerous factors. Changes in orientation, dynamics, and tensor parameters all lead to modifications of the chemical shift. Indeed, the chemical shift tensor has been shown to be sensitive to the neighboring amino acids and the polypeptide secondary structure (*1–3*), the H-bonding strength (*4, 5*), protonated versus deprotonated states (*6, 7*), and ion-binding (*8*). Two different crystal forms of Boc-glycylglycylglycine benzyl ester revealed large differences in their chemical shift tensor elements despite having very similar isotropic chemical shifts (*9*). Here, we show that changes in the observed chemical shifts of an oriented membrane-bound polypeptide, gramicidin A, upon cation binding are due to the electronic shielding effect, i.e., changes in the magnitudes of the chemical shift tensor elements. With the principal values determined in the presence of cations, the observed changes in ^{15}N chemical shifts in oriented samples upon cation binding are reproduced from the known structure without modifying the structure or dynamics of the polypeptide significantly.

The analysis of anisotropic chemical shifts is being used in the characterization of many different proteins (melittin (*10*); colicin (*11*); fd coat protein (*12*); M2 protein from influenza A virus (*13*)), protein ligand interactions (bacteriorhodopsin (*14*)), and polypeptides (gramicidin (*15*); alamethicin (*16*)). Consequently, a detailed characterization of these spin interaction tensors is essential, as well as an understanding of the factors that influence the observed values in oriented samples.

Gramicidin A, a pentadecapeptide, is an enzymatic product of the bacterium *Bacillus brevis.* One of its biological roles is to induce cell lysis in neighboring organisms by forming a channel that conducts monovalent cations and water across membranes (*17*). The transmembrane channel form of gramicidin A is an amino terminus to amino terminus single-stranded dimer, and each monomer is a right-handed β-helix with 6.5 residues per turn (*18*, pdb: #1mag). The gramicidin A channel is monovalent cation selective: small monovalent cations permeate the 4-Å diameter pore, divalent cations bind and block, and anions are rejected. A pair of symmetrically located ion-binding sites were found by X-ray diffraction for Tl^+ at 9.6 ± 0.3 Å and for Ba^{2+} at 13.0 ± 0.2 Å from the midpoint of the gramicidin A channel (*19*). Details of the delocalized monovalent cation binding sites and the cation solvation environment have been emerging (*20*). A comparison of the structure and dynamics of the gramicidin A channel in the absence and presence of cations will provide insight as to how the channel functions, but such a comparison is dependent on interpreting chemical shifts of oriented samples accurately.

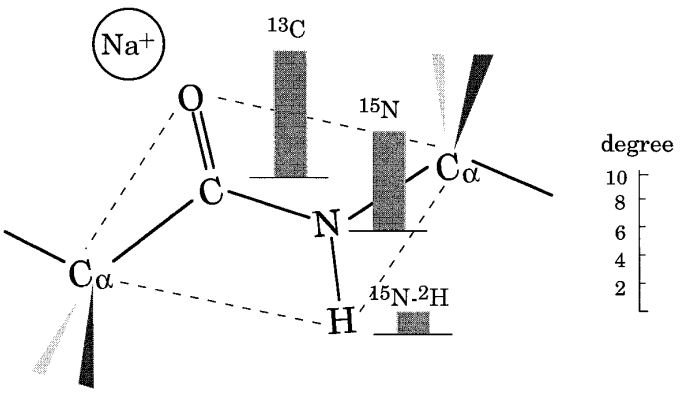

FIG. 1. Schematic representation of predicted changes in the mean orientation of the peptide plane about the C_α–C_α axis calculated from the observed changes of different anisotropic spin interactions for the Leu_{12}–Trp_{13} peptide plane. These calculations are based on the assumption that the changes in the NMR observables are caused by structural deformation alone.

1090-7807/98 $25.00

TABLE 1

Orientational Constraints of Leu_{12}–Trp_{13} and Trp_{11}–Leu_{12} Sites of gA Channel Observed in the Absence and Presence of Cations

Backbone sites	^{15}N chemical shift (±1 ppm)[a]	Dipolar splitting (±40 Hz) ^{15}N–^{2}H[a,b]	Dipolar splitting (±40 Hz) ^{13}C–^{15}N[b,c]
Leu_{12}–Trp_{13}			
Without Na^+	184.5	3034 (12.2°)	514 (46.8°)
With Na^+	178.5	2985 (13.6°)	471 (47.5°)
With K^+	174.5	2888 (15.3°)	
Trp_{11}–Leu_{12}			
Without Na^+	134.0	2228 (27.5°)	
With Na^+	132.0	2232 (27.5°)	

[a] From Ref. (*20*).

[b] The angular interpretations represent the angle between the covalent bond and the magnetic field direction.

[c] New orientational constraints.

In our previous study (*20*), it was shown that the ^{15}N chemical shift of several residues in uniformly aligned sample preparations of gramicidin A changes significantly upon Na^+ binding. However, it was rationalized that these changes were not the result of the anticipated structural changes induced by cation binding. These observations are illustrated for the Leu_{12}–Trp_{13} peptide plane in Fig. 1. A change of 50 Hz out of 3 kHz was observed for the ^{15}N–^{2}H dipolar interaction upon adding enough Na^+ to achieve 80% double occupancy based on known binding constants (*17*). A 6-ppm change in ^{15}N chemical shift is observed under similar conditions, and a 7-ppm change in $^{13}C_1$ chemical shift has been extrapolated from the results of Cornell and co-workers (*21*). Data on this and the Trp_{11}–Leu_{12} sites are presented in Table 1. For this latter site and indeed for all even sites (identified by the residue number of the amide nitrogen), there is no significant change in the NMR observables. The change in the anisotropic spin interactions for the Leu_{12}–Trp_{13} site is interpreted for Fig. 1 as a change in mean orientation of the peptide plane about the C_α–C_α axis. The inconsistent result suggests that the induced change in chemical shift for these oriented samples is not due to a structural change, but rather a change in the chemical shift tensor.

Furthermore, the $^{13}C_1$–^{15}N dipolar interaction of the $^{13}C_1$–Leu_{12}–^{15}N–Trp_{13} labeled site was measured with and without Na^+ present (Table 1). With the additional constraints, it is possible to expand the structural deformation model (Fig. 2A). Here we consider both a rotation of the peptide plane about the

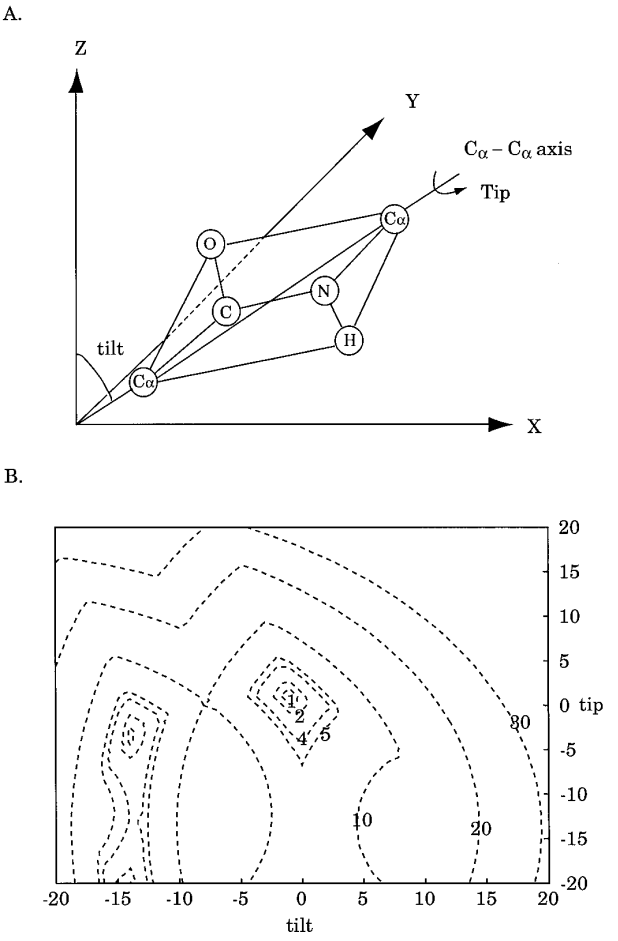

FIG. 2. (A) Model for the structural deformation of peptide plane in gramicidin A upon Na^+ binding. "Tip" is defined as the rotation of the peptide plane around the C_α–C_α axis, while "tilt" is defined as the orientation of the C_α–C_α axis with respect to the magnetic field direction and the channel axis. (B) The ^{15}N–^{2}H and ^{13}C–^{15}N dipolar interactions were calculated for tip and tilt angles of the Leu_{12}–Trp_{13} peptide plane using −20° to 20° from the experimentally defined structure in the absence of cations. The sum of the absolute differences between the calculated and the observed dipolar splittings in the presence of Na^+ scaled with respect to the experimental error are plotted for each tip and tilt pair. Contours at 1, 2, 4, 5, 10, 20, 30 are shown. This plot gives two minima: one is at tip 1°, tilt −1° and another at tip −3°, tilt −14°.

TABLE 2

Structural Influence on the NMR Observables from the Leu_{12}–Trp_{13} Peptide Plane

	No cations	Na^+	K^+
Anisotropic ^{15}N chemical shift (ppm)	184.5	178.5	174.5
Structural deformation		tip = 1° tilt = −1°	tip = 4° [d]tilt = 0°
Calculated anisotropic ^{15}N chemical shift (ppm)		[a]182.8 [b]178.9	[a]182.8 [c]175.7

[a] Based on σ_{11} = 45.5, σ_{22} = 68.0, and σ_{33} = 199.5 ppm, and the structural deformations defined by the dipolar interaction results.

[b] Based on σ_{11} = 47, σ_{22} = 68.0, and σ_{33} = 195 ppm, and the structural deformations defined by the dipolar interaction results.

[c] Based on σ_{11} = 45, σ_{22} = 71, and σ_{33} = 193.5 ppm, and the structural deformations defined by the dipolar interaction results.

[d] ^{15}N–^{13}C dipolar data are not available.

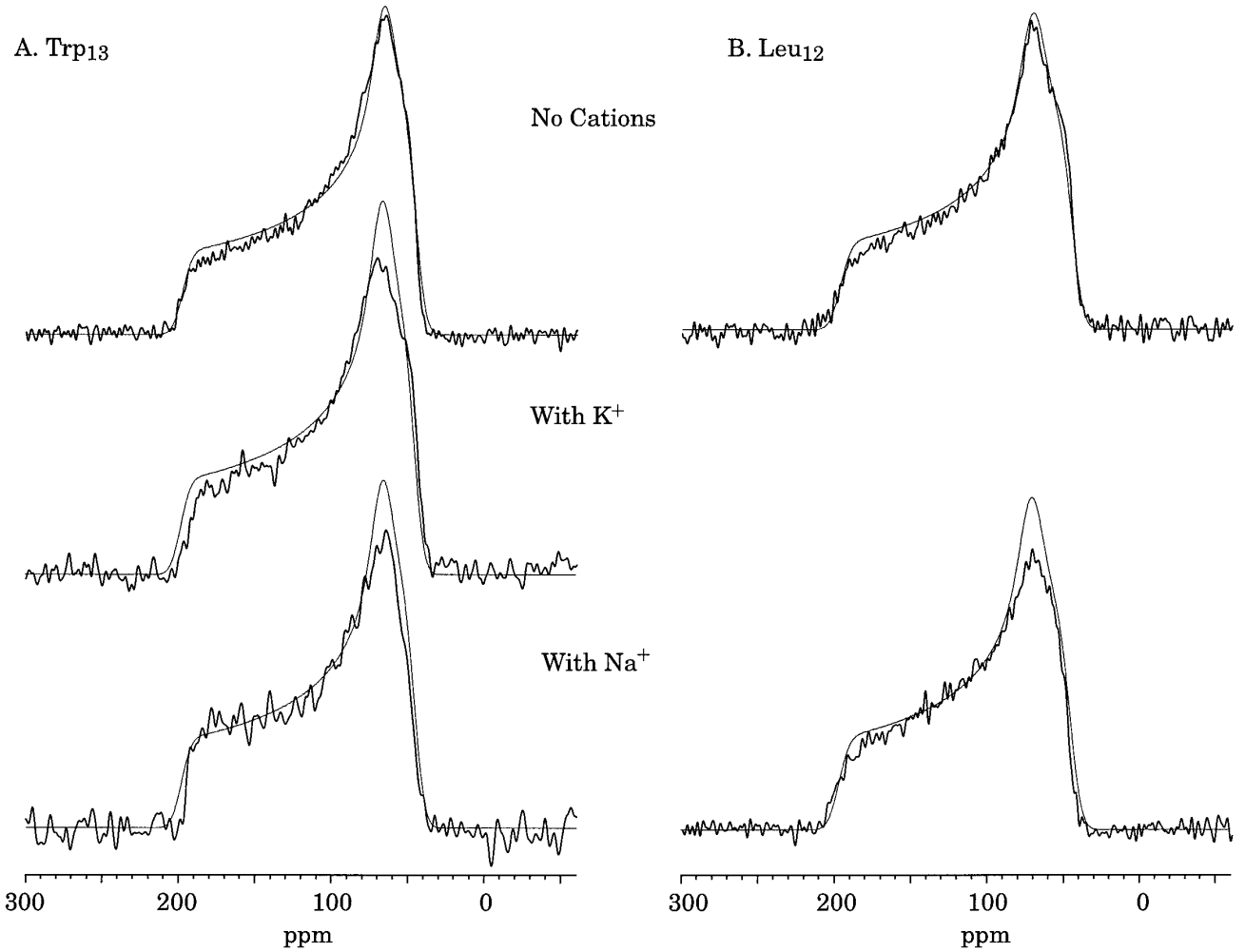

FIG. 3. ^{15}N chemical shift powder pattern spectra of gramicidin A (80 mg) in hydrated DMPC bilayers (peptide:lipid molar ratio 1:8) acquired at 276 K. (A) $^{15}N_{\alpha}$–Trp_{13}; (B) $^{15}N_{\alpha}$–Leu_{12}. Samples were hydrated with water (50% by weight) or aqueous salt solutions so that more than 80% double occupancy was achieved. For detailed sample preparation procedure, see (*23*). The thinner lines correspond to the best simulation of the spectra without cations present. Spectra were recorded at 40.585 MHz using a home-built NMR spectrometer with a Chemagnetics data acquisition system. Typical parameters for these experiments were 6-μs 90° pulse; 1-ms contact time; 50-μs Hahn echo delay, and 12-s recycle delay. Data were processed using Spinsight software (Chemagnetics) with minimal Gaussian line broadening to preserve the discontinuities of the powder spectra, usually between 50 and 100 Hz. The spectral simulations were performed on a Silicon Graphics workstation using the program TENSORI developed in our lab.

C_{α}–C_{α} axis, defined as tip, and a change in the orientation of this axis with respect to the channel axis, defined as tilt. Since the Leu_{12}–Trp_{13} peptide plane is nearly parallel to the channel axis, the ^{15}N–^{2}H dipolar interaction is sensitive to the tip, but not very sensitive to the tilt while the ^{13}C–^{15}N dipolar interaction is sensitive to the tilt but not very sensitive to the tip. The ^{15}N–^{2}H and ^{13}C–^{15}N dipolar splittings are calculated over a range of the tip and tilt angles of the peptide plane and compared with the experimental observations when the channel has 80% double occupancy with Na^{+}. In Fig. 2B, the absolute differences between the calculated and observed values which are scaled with respect to the experimental error (and are therefore unitless) are plotted as a function of the tip and tilt angles of the Leu_{12}–Trp_{13} plane relative to angles when no cations are present. This plot gives two minima: one is at $-3°$ tip, $-14°$ tilt and the other at 1° tip, $-1°$ tilt. However, a change of 14° in the tilt angle is inconsistent with the observed chemical shift values. The ^{15}N chemical shift is more sensitive to tilt than tip and in Fig. 1 it is noted that the chemical shift change for this site was consistent with a tip of 7°; therefore it would be consistent with only a tilt angle much smaller than 14°. Therefore, a 1° change in tip and tilt is the correct solution. Such small changes in structure do not account for the relatively large observed changes in chemical shift. The predicted chemical shifts from this small structural modification are presented in Table 2.

Figure 3 shows the ^{15}N chemical shift powder pattern spectra of gramicidin A in hydrated DMPC (dimyristoylphosphatidylcholine) bilayers recorded at 276 K. Samples were hydrated with water or aqueous salt solutions so that 80% double occu-

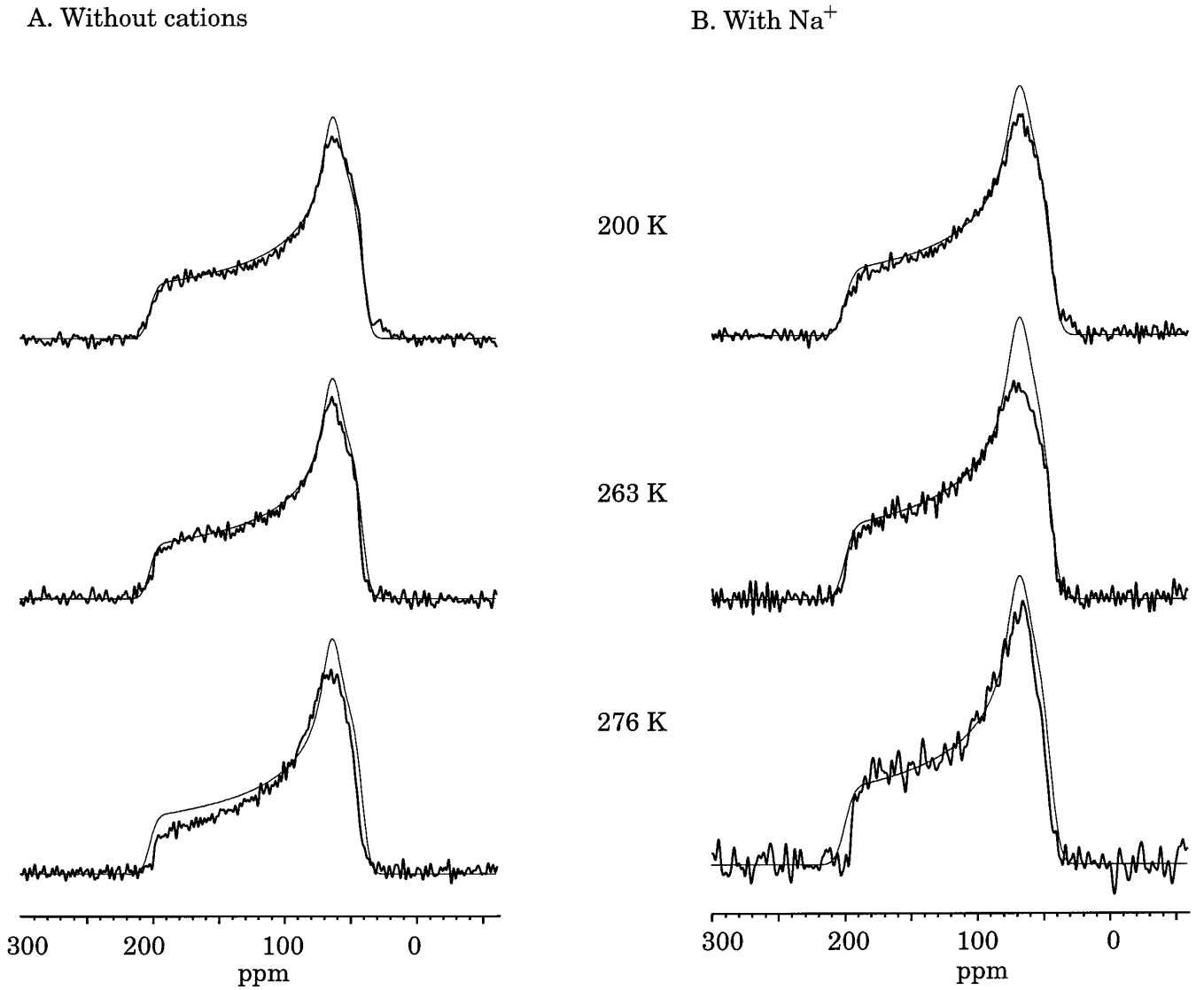

FIG. 4. ^{15}N chemical shift powder spectra of fast frozen $^{15}N_{\alpha}$–Trp_{13} gA/DMPC hydrated with water or NaCl solution acquired at 200, 263, and 276 K. The thinner lines correspond to the best simulation of the static spectrum recorded at 200 K. Fast freezing was performed by plunging thin films of the hydrated powder into liquid propane at 85 K. The frozen films were transferred to an NMR tube submersed in liquid nitrogen. This was done in a glove bag filled with nitrogen gas to avoid condensation on the surface of the frozen sample. Once the entire sample was transferred, the tube was sealed and kept in liquid nitrogen until positioned in the precooled solid state NMR probe for observation. Nitrogen boil-off gas was used for temperature regulation in all low temperature experiments. The sample temperature was measured by a thermocouple mounted at the end of a home-built variable temperature stack 3.8 cm from the center of the coil. In order to minimize RF sample heating during the acquisition time, a high flow rate (>800 1/hr) of cooling gas was maintained, and short acquisition time (7 ms) with a long recycle delay (12 s) was used. Good temperature control was indicated by little change in the probe tuning during the experiments.

pancy could be achieved. The global rotational diffusion around the channel axis ceases at this temperature (*22*); therefore the chemical shift powder patterns were only averaged by local motions. The magnitudes of the chemical shift tensor elements were extracted from chemical shift powder pattern simulations. For the $^{15}N_{\alpha}$–Trp_{13} site (Fig. 3A), the principal values of the chemical shift tensor are 45.5, 68.0, and 199.5 ppm without cations present; 45.0, 71.0, and 193.5 ppm in the presence of K^+; and 47.0, 68.0, and 195.0 ppm in the presence of Na^+. The experimental error bars are ± 1.5 ppm. Significant changes in the σ_{33} tensor element of 6 and 4.5 ppm by the binding of K^+ and Na^+, respectively, were observed. For the $^{15}N_{\alpha}$–Leu_{12} site (Fig. 3B), the principal values of the chemical shift tensor are 43.0, 69.0, and 195.0 ppm without cations present and 45.0, 69.0, and 197.0 ppm in the presence of Na^+. No significant change in the magnitudes of the tensor elements was observed.

The observed shift in the σ_{33} tensor element (for Trp_{13}) when cations bind may result from changes in the static principal values of the chemical shift tensor and/or a change in the

TABLE 3

Magnitudes of the Chemical Shift Tensor Elements (ppm) for $^{15}N_{\alpha}$–Trp_{13} gA/DMPC in the Absence and Presence Na^+ at Concentrations Sufficient to Achieve 80% Double Occupancy

T(K)	σ_{33}	σ_{22}	σ_{11}
200			
Without Na^+	204	65.5	42.5
With Na^+	199	67	43
263			
Without Na^+	201	66	43.5
With Na^+	198	68	43.5
276			
Without Na^+	199.5	68	45.5
With Na^+	195	68	47

dynamics of the observed site. A series of chemical shift powder pattern spectra of $^{15}N_{\alpha}$–Trp_{13} gramicidin A in lipid bilayers with and without Na^+ present have been acquired at 200, 263, and 276 K, shown in Fig. 4. A fast frozen sample preparation technique has been employed to prevent the formation of large ice crystals and distortion of the lipid bilayers by going below the gel to liquid crystalline phase transition; thereby conformational heterogeneity is avoided and the discontinuities of the powder pattern can be well preserved (*23*). At 200 K, the peptide plane librational motion ceases, and the static principal values of the chemical shift tensor can be obtained. While the σ_{11} and σ_{22} tensor elements are insensitive to cation binding, the σ_{33} tensor element shifts upfield by 5 ppm (Table 3). The local motion of the peptide plane has been modeled as a rotation around the C_{α}–C_{α} axis from analyzing the chemical shift powder patterns recorded at different temperatures without cations present (*24*). The similar motional average of the tensor element magnitudes in the presence and absence of Na^+ (Table 3) indicates that there is little change, if any, in the dynamics of gramicidin A upon Na^+ binding. In fact, little change in the ^{15}N–^2H dipolar splitting upon cation binding also implies that there is no significant change in dynamics. This latter point is important because of the near alignment ($\sim$15°) of the unique axis of the dipolar interaction tensor and the dominant ^{15}N chemical shift tensor element σ_{33} (*25*). A librational motion of the peptide plane around the C_{α}–C_{α} axis or indeed virtually any axis would average the σ_{33} tensor element and ^{15}N–^2H dipolar interaction to a similar extent. Since this was not observed and since the averaging of the CSA is similar in the presence and absence of cations it is argued here that dynamics do not account for the observed changes in the anisotropic chemical shifts.

With both the structural and dynamic influence on the anisotropic chemical shifts accounted for, it is now possible to recalculate the chemical shifts using the *in situ* experimentally defined principal values of the chemical shift tensor and the experimentally defined small change in structure. Predicted chemical shifts within the experimental error limits are achieved (Table 2). The complexity in interpreting changes in anisotropic chemical shifts are clearly demonstrated, and yet the change in the ^{15}N chemical shift principal elements induced by cation binding to the carbonyl oxygens are not large. Greater changes in the principal elements have previously been observed in a study of Cs^+-promoted silver catalyst (*8*). While the changes are relatively small ($<$10 ppm) here, they were defined within a small error bar due to high signal-to-noise spectra from these membrane-bound polypeptide samples and by having the dynamics characterization substantially enhanced by the fast freezing methodology. Through this effort the observed changes in principal elements provide additional evidence for the hypothesized indirect polarizability effect: by binding to the carbonyl oxygen, cations have indirectly polarized, by a through-bond effect, the carbonyl carbon and the amide nitrogen of the peptide planes.

While a modest change is reported here for the principal elements of the chemical shift tensor, even smaller effects on structure result from cation binding. The lack of a structural change has not been adequately modeled by molecular dynamics. Indeed, molecular dynamics calculations have predicted structural deformations as great as 40° for the tip of the peptide plane (*26*). Moreover, a molecular modeling study based on NMR orientational constraints suggests that an ideal solvation environment for the cation inside the channel is not achieved as a result of the lack of structural deformation (*27*). Such solvation while anticipated is not desired since it would generate a deep potential energy well in the translocation pathway for cation passage across membranes, consequently slowing down the transport process.

ACKNOWLEDGMENTS

We are indebted to R. Rosanske and A. Blue for their skillful maintenance and service of the NMR spectrometers and to H. Henricks and U. Goli for their assistance with peptide synthesis. T.A.C. gratefully acknowledges support from the National Science Foundation (DMB 9603935), and the work was largely performed at the National High Magnetic Field Laboratory supported by NSF Cooperative Agreement DMR-9527035 and the state of Florida.

REFERENCES

1. T. G. Oas, C. J. Hartzell, F. W. Dahlquist, and G. P. Drobny, The amide ^{15}N chemical shift tensors of four peptides determined from ^{13}C dipole-coupled chemical shift powder patterns, *J. Am. Chem. Soc.* **109,** 5962–5966 (1987).
2. T. G. Oas, C. J. Hartzell, T. J. McMahon, F. W. Dahlquist, and G. P. Drobny, The carbonyl ^{13}C chemical shift tensors of five peptides determined from ^{15}N dipole-coupled chemical shift powder patterns, *J. Am. Chem. Soc.* **109,** 5956–5962 (1987).
3. C. J. Hartzell, M. Whitfield, T. G. Oas, and G. P. Drobny, Determination of the ^{15}N and ^{13}C chemical shift tensors of L-[^{13}C]alanyl-L-[^{15}N]alanine from the dipole-coupled powder patterns, *J. Am. Chem. Soc.* **109,** 5966–5969 (1987).
4. N. Asakawa, S. Kuroki, H. Kurosu, I. Ando, A. Shoji, and T. Ozaki, Hydrogen-bonding effect on ^{13}C NMR chemical shift of L-alanine

residue carbonyl carbons of peptides in the solid state, *J. Am. Chem. Soc.* **114,** 3261–3265 (1992).

5. S. Kuroki, S. Ando, and I. Ando, Hydrogen-bonding effect on ^{15}N NMR chemical shift of the glycine residue of oligopeptides in the solid state as studied by high-resolution solid-state NMR spectroscopy, *J. Mol. Struct.* **240,** 19–29 (1990).
6. G. Harbison, J. Herzfeld, and R. G. Griffin, Nitrogen-15 chemical shift tensors in L-histidine hydrochloride monohydrate, *J. Am. Chem. Soc.* **103,** 4752–4754 (1981).
7. M. Munowitz, W. W. Bachovchin, J. Herzfeld, C. M. Dobson, and R. G. Griffin, Acid-base and tautomeric equilibria in the solid state: ^{15}N NMR spectroscopy of histidine and imidazole, *J. Am. Chem. Soc.* **104,** 1192–1196 (1982).
8. X. Wang and P. Ellis, Cesium-induced structural change of absorbed ethylene on cesium-promoted silver catalyst studied by ^{13}C solid state nuclear magnetic resonance, *J. Am. Chem. Soc.* **113,** 9675–9676 (1991).
9. Y. Hiyama, C. Niu, J. V. Silverton, A. Bavoso, and D. A. Torchia, Determination of ^{15}N chemical shift tensor via ^{15}N–^{2}H dipolar coupling in Boc-glycylglycyl[^{15}N]glycine Benzyl ester, *J. Am. Chem. Soc.* **110,** 2378–2383 (1988).
10. R. Smith, F. Separovic, T. J. Milne, A. Whittaker, F. M. Bennett, B. A. Cornell, and A. Makriyannis, Structure and orientation of the pore-forming peptide, melittin, in lipid bilayers, *J. Mol. Biol.* **241,** 456–466 (1994).
11. Y. Kim, K. Valentine, S. J. Opella, S. L. Schendel, and W. A. Cramer, Solid-state NMR-studies of the membrane-bound closed state of the Colicin E1 channel domain in lipid bilayers, *Protein Sci.* **7,** 342–348 (1998).
12. F. M. Marassi, A. Ramamoorthy, and S. J. Opella, Complete resolution of the solid state NMR spectrum of a uniformly ^{15}N-labeled membrane protein in phospholipid bilayers, *Proc. Natl. Acad. Sci.* **94,** 1739–1744 (1997).
13. F. A. Kovacs and T. A. Cross, Transmembrane four-helix bundle of influenza A M2 protein channel: Structural implications from helix tilt and orientation, *Biophys. J.* **73,** 2511–2517 (1997).
14. A. S. Ulrich, M. P. Heyn, and A. Watts, Structure determination of the cyclohexene ring of retinal in bacteriorhodopsin by solid-state NMR, *Biochemistry* **31,** 10,390–10,399 (1992).
15. L. K. Nicholson and T. A. Cross, Gramicidin cation channel: An experimental determination of the right-handed helix sense and verification of β-type hydrogen bonding, *Biochemistry* **28,** 9379–9385 (1989).
16. C. L. North, M. Barranger-Mathys, and D. Cafisco, Membrane orientation of the N-terminal segment of alamethicin determined by solid-state ^{15}N NMR, *Biophys. J.* **69,** 2392–2397 (1995).
17. D. D. Busath, The use of physical methods in determining gramicidin channel structure and function, *Annu. Rev. Physiol.* **55,** 473–501 (1993).
18. R. R. Ketchem, B. Roux, and T. A. Cross, High-resolution polypeptide structure in a lamellar phase lipid environment from solid state NMR derived orientational constraints, *Structure* **5,** 1655–1669 (1997).
19. G. A. Olah, H. W. Huang, W. H. Liu, and Y. L. Wu, Location of ion-binding sites in the gramicidin channel by X-ray diffraction, *J. Mol. Biol.* **218,** 847–858 (1991).
20. F. Tian, K.-C. Lee, W. Hu, and T. A. Cross, Monovalent cations transport: Lack of structural deformation upon cation binding, *Biochemistry* **35,** 11,959–11,966 (1996).
21. R. Smith, D. E. Thomas, A. R. Atkins, F. Separovic, and B. A. Cornell, Solid-state ^{13}C-NMR studies of the effects of sodium ions on the gramicidin A ion channel, *Biochim. Biophys. Acta* **1026,** 161–166 (1990).
22. K. C. Lee, W. Hu, and T. A. Cross, ^{2}H NMR determination of the global correlation time of the gramicidin channel in a lipid bilayer, *Biophys. J.* **65,** 1162–1167 (1993).
23. N. D. Lazo, W. Hu, K. C. Lee, and T. A. Cross, Rapidly-frozen polypeptide samples for characterization of high definition dynamics by solid-state NMR spectroscopy, *Biochem. Biophys. Res. Commun.* **197,** 904–990 (1993).
24. N. D. Lazo, W. Hu, and T. A. Cross, Low-temperature solid-state ^{15}N NMR characterization of polypeptide backbone librations, *J. Magn. Reson. B* **107,** 43–50 (1995).
25. W. Mai, W. Hu, C. Wang, and T. A. Cross, Orientational constraints as three-dimensional structural constraints from chemical shift anisotropy: The polypeptide backbone of gramicidin A in a lipid bilayer, *Protein Sci.* **2,** 532–542 (1993).
26. D. H. Mackay, P. H. Berens, K. R. Wilson, and A. T. Hagler, Structure and dynamics of ion transport through gramicidin A, *Biophys. J.* **56,** 229–248 (1984).
27. F. Tian and T. A. Cross, Cation transport—An example of structural based selectivity, submitted.